International Journal of Concrete Structures and Materials

RESEARCH

Open Access

Performance of Self-healing Cementitious Mortar with PVA Fiber and SAP

Sukmin Kwon[1], Sugyu Lee[1], Hyunuk Kang[2], Min Kyoung Kim[3], Sungwun Her[4], Sungchul Bae[4], Dong Joo Kim[3] and Juhyuk Moon[2*]

Abstract

Although concrete materials generally exhibit outstanding mechanical properties, it is susceptible against crack formation. It has been reported that narrow cracks (≤ 150 μm) could be naturally sealed in the cement matrix by externally supplied water-induced hydration. However, the crack width of larger than 150 μm is difficult to be sealed without using additional self-healing admixture. In this study, the self-healing cementitious mortar was successfully developed by using a combination of polyvinyl alcohol (PVA) fiber and superabsorbent polymer (SAP), aiming to heal the wide cracks. Although the mechanical properties were slightly reduced, it shows outstanding self-healing performance by using the dual admixtures. A self-healing rate of 60% was observed in the control sample with an initial crack width of 300 μm, while a self-healing rate of nearly 100% was confirmed with suitable SAP and PVA. In addition, it was confirmed that lower hydration degree of self-healing mortar in early stage contributes to the enhanced self-healing performance of developed composite system by internally supplied water from SAP.

Keywords Self-healing, Mortar, Evaluation, Cement hydration, Internal curing

1 Introduction

Concrete is one of the mostly used man-made materials in the world (Gagg, 2014). Since concrete has excellent mechanical properties, it is widely used in various applications (Branco & Mendes, 1993; Gustavsson & Sathre, 2006; Stewart et al., 2011). However, it possesses durability issues (i.e., penetration of chloride ions and water induced by crack formation). It can cause problems including a rise in the maintenance costs for the concrete structure and an increase in user anxiety and discomfort (Chindasiriphan et al., 2020; Gardner et al., 2018). Hence, self-healing concrete which can seal newly formed cracks, has been actively developed, recently (Talaiekhozani & Abd Majid, 2014).

The self-healing mechanisms of concrete have been generally reported as continued hydration or swelling of unreacted particles (Jacobsen & Sellevold, 1996; Reinhardt & Jooss, 2003; Termkhajornkit et al., 2006; Yang et al., 2009). There are two potential hydration mechanisms that can address the self-healing behavior in cementitious materials: autogenous crack sealing effect by the precipitation of calcium silicate hydrate (C–S–H) and calcium carbonate ($CaCO_3$). These autogenous crack healing are easily occurred in some specific environments such as presence of Ca^{2+} and CO_2, humid conditions (continuous water supply), and small crack widths (Tittelboom & Belie, 2013). The self-healing efficiency of Ordinary Portland cement (OPC) was reported to be effective only in a relatively narrow crack width (≤ 150 μm) (Yang et al., 2009). To maximize the self-healing effect for wider

Journal information: ISSN 1976-0485 / eISSN 2234-1315

*Correspondence:
Juhyuk Moon
juhyukmoon@snu.ac.kr
[1] Land and Housing Institute, Korea Land and Housing Corporation, 99, Expo-Ro, Yuseong-Gu, Daejeon 34047, Republic of Korea
[2] Department of Civil and Environmental Engineering, Seoul National University, Seoul 08826, Republic of Korea
[3] Department of Civil and Environmental Engineering, Sejong University, 209, Neungdong-Ro, Gwangjin-Gu, Seoul 05006, Republic of Korea
[4] Department of Architectural Engineering, Hanyang University, 222, Wangsimni-Ro, Seongdong-Gu, Seoul 04763, Republic of Korea

crack width, the additional methods have to be adopted (Li & Li, 2011; Li et al., 1998; Tittelboom & Belie, 2013). For example, encapsulation methods were frequently used (Tittelboom et al., 2010, 2011). With this approach, a material that can improve the self-healing performance of concrete is placed in a tube. In other words, when a crack occurs in the concrete, the tube is simultaneously broken, creating an environment in which the concrete can seal the crack region. After the crack is propagated into the concrete, another tube also got cracked, and glue released into the crack (Joseph et al., 2007; Mihashi et al., 2000).

Another potential admixture for making self-healing concrete is superabsorbent polymer (SAP) (Chindasiriphan et al., 2020; Lee et al., 2010, 2016; Snoeck et al., 2012). Since this material has ability of absorbing a significant amount of liquid, it can reduce self-desiccation shrinkage and furthermore, promote an internal curing effect by supplying water in later hydration stage (Jensen & Hansen, 2002). Based on this mechanism, the SAP can fill the crack parts in concrete as it releases the pre-absorbed water into the cement matrix (Lee et al., 2016). In addition, polyvinyl alcohol (PVA) fibers are also used as self-healing materials (Li et al., 2002; Nasim et al., 2020; Şahmaran & Li, 2009). Homma et al., reported that cracks less than 100 μm in cement matrix is almost completely recoverable. Specifically, short-length fibers with random distribution are the most suitable to control crack width and heal cracks in concrete (Homma et al., 2009). When the PVA is embedded in concrete, it can reduce the width of cracks occurring in concrete so the self-healing performance can be more substantial (Jonkers et al., 2010). Furthermore, the crystallization products can be easily deposited on the PVC fiber nearby cracks due to hydroxyl groups attracts calcium ions (Jonkers et al., 2010).

Although lots of previous studies have been reported on the self-healing performance of concrete using SAP and PVA individually, systematic studies evaluating the self-healing performance of concrete using a combination of the two materials are limited (Tittelboom & Belie, 2013). In addition, there are few previous studies on self-healing performance for relatively wide crack widths ($\geq$150 μm) and accurate evaluation of the self-healing performance of cementitious materials. Therefore, the purpose of this study is to investigate the effect of SAP and PVA on the self-healing performance of mortar focused on the healing ability for a wide crack width (e.g., 300 μm). A series of experiments of X-ray diffraction (XRD), thermogravimetric analysis (TGA), isothermal calorimetry, optical microscopy, leaking test, and micro-X-ray computed tomography (micro-CT) was performed to evaluate the self-healing performance and elucidate the self-healing mechanism.

2 Materials and Experimental Methods

2.1 Materials and Sample Preparations

In this study, type 1 OPC with a fineness (Blaine) of 3570 cm^2/g, polyacrylic acid-co-acrylamide SAP, PVA fiber, and silica sand were used as raw materials. The SAP, which induces the absorption and release of moisture, has an average particle size of 1118 μm and a specific gravity of 0.6 to 0.8 g/cm^3. Additionally, the PVA fiber with a tensile strength of 1200 MPa has a length of 3 mm and an average diameter of 0.022 mm. In particular, by using PVA together with SAP, resistance to crack formation can be increased. These additional self-healing products can serve as a bridge to fill the cracks. In the case of sand used for mortar, the well graded sand with a particle size of 0.42–2.36 mm was mixed at a ratio of 2.4 to that of cement. The X-ray fluorescence (XRF) results on raw materials are shown in Table 1.

The mix design of self-healing mortar is shown in Table 2. In the case of a self-healing mortar with a water–cement ratio of 0.45, a large amount of water reducing agent was required. To prevent adverse reactions such as strength reduction and delayed hydration due to the initial water absorption by SAP, additional water was incorporated. Based on the flow diameter of control in which a very small amount of water reducing agent was incorporated, the amount of extra water was considered based on the flow value of reference sample. In the process of mixing the self-healing mortar, OPC, silica sand, SAP, and PVA were dry mixed for 1 min. Subsequently,

Table 1 X-ray fluorescence results of raw materials

Formula (unit %)	OPC	PVA	SAP
CaO	58.8	–	–
SiO_2	20.0	0.1	0.1
Al_2O_3	5.0	–	–
MgO	3.9	0.1	–
Fe_2O_3	3.2	–	–
SO_3	2.4	0.1	0.2
K_2O	1.2	–	0.1
TiO_2	0.2	–	–
P_2O_5	0.2	–	–
MnO	0.01	–	–
ZnO	0.1	–	–
SrO	0.1	–	–
Na_2O	–	0.1	13.7
Martix	–	99.6	85.9
Lol	4.8	–	–

Table 2 Mix design and flow results

Notation	Cement	Water	Sand	SAP	PVA (vol%)	Super plasticizer	Extra water	Flow (mm)
Control	1.0	0.45	2.4	–	–	0.0026	–	185
S05F25				0.005	0.25		0.0233	185
S05F50					0.5		0.0500	183
S10F25				0.01	0.25		0.0467	183
S10F50					0.5		0.0700	183
S30F25				0.03	0.25		0.1400	185
S30F50					0.5		0.1900	185

the premixed powder and water were mixed by a mortar mixer for 5 min.

Next, paste samples were prepared for the isothermal calorimetry experiments, XRD, and TGA test. All raw materials (OPC, SAP, and superplasticizer) were mixed in dry condition for 1 min and then the powder mixture was mixed with water for 5 min. Thereafter, they were cured for 3, 7, 14, and 28 days under the same curing conditions as the mortar specimens described above.

To analyze the self-healing performance, the optical microscopic analysis and leaking test were conducted with the mortar samples. Firstly, three replicate cylinder specimens with a dimension (diameter: 50 mm and height: 100 mm) were prepared for each variable. Then the specimens were cured in water for 7 days at a temperature of 20 °C. Subsequently, crack widths of 100, 200, and 300 μm were generated by performing a split tensile test after curing under water for 7 days. The 0.1-mm-thick silicone sheet(s) were employed to control the crack width of the specimens, and the circumference of the stainless band was carefully adjusted until the desired crack width was achieved. As for the specimens for micro-CT measurements, three downsized cylindrical specimens (diameter: 25 mm and height: 25 mm) were prepared in the same procedure as above, and cracks (width: 200 μm) were introduced and controlled.

2.2 Experimental Details

Flexural and compressive strength tests were conducted to examine the effect of the incorporation of self-healing materials on mechanical strength of mortar samples. The slurry was placed into the $40 \times 40 \times 160$ mm^3 molds (Kang & Moon, 2021). The curing conditions of the samples were as follows. After casting, the slurry was cured in the condition of 20 °C for 1 day. And then, the samples were demolded. Lastly, the samples were cured under water until the designated curing period. For mechanical strength at 3, 7, 14, and 28 curing days, three mortar samples for each variable were measured. The loading speed was controlled by the speed increment rate and was set to 50 ± 10 N/s for the flexural strength test and 2400 ± 200 N/s for the compressive strength test.

The isothermal calorimetry experiments were performed using the device (TAM Air 8-channel, TA Instruments, New Castle, DE, USA) to analyze the hydration reaction in the early stage (Jansen et al., 2012). The heat normalization using aggregate was performed considering the specific heat of OPC, water, and self-healing materials. The paste was used, and the measurement start point was precisely set to 2 min after the mixing started. Before the measurement finished, heat flow was stabilized for 1 h (Kang et al., 2021). Based on the preliminary tests, the reproducibility of the conducted test method was verified.

For XRD and TG analyses, the paste samples cured for 3, 7, 14, and 28 days were pulverized for 10 min. Subsequently, to apply the hydration stop method, the fine powders emerged for 30 min in isopropyl alcohol and ethyl ether, respectively. And then, the obtained powder was dried in the condition of 40 °C for 40 min (Jeong et al., 2019). The XRD experiments were performed with an X-ray diffractometer (D2 PHASER, Bruker Co. Ltd., Land Baden-Württemberg, Germany). The measurement range was set from 5° to 60°, and the Cu-k α ($\lambda = 1.5418$ Å) radiation source was adopted (Jeong et al., 2018; Kang & Moon, 2021). TG analysis (TGA) measurement was conducted with a DSC/TG system (SDT Q600, TA Instrument Ltd., Newcastle, DE, USA). The 10 K/min of heating rate was selected, and the temperature range was set from 20 to 1050 °C (Kang et al., 2022). The chemically bound water (CBW) value was assigned as weight loss at 600 °C, and the amount of calcium hydroxide was calculated based on the difference between 400 and 500 °C (Deboucha et al., 2017; Jeong et al., 2015).

For optical microscopic measurement, the self-healing performance was evaluated by surface observation (AM7515MZT, Dino-Lite, USA). Surface crack width according to the curing duration of 0, 3, 7, 14, and 28 days after crack formation was recorded by image processing (Shin et al., 2020). Three specimens per one variable were

measured, and five points per specimen were recorded to obtain reliable data collection. For the leaking test, a 200-mm-height acrylic pipe was used to measure the leaked amount of water for 10 min. If all water was discharged within 10 min, the total leaking time (i.e., less than 10 min) was recorded. Subsequently, the amount of water leaked through the crack was measured at the curing dates of 0, 3, 7, 14, 28, 56, and 91 days, respectively.

From the use of micro-CT, it is possible to analyze the pore properties of cementitious materials (Pae et al., 2021a), and a tomography scanner (SkyScan 1272, Bruker Belgium, Kontich, Belgium) was utilized. 0.11 mm Cu energy filter equipped with a certain current (100 μA) and voltage (100 kV) were selected for obtaining the spatial resolution of 8 μm/pixel with 2452×2452 pixels (Pae et al., 2021b). After micro-CT measurement, the crack region was segmented for calculating the largest connected area in binary images.

3 Results

3.1 Compressive Strength Results

The compressive strength results with average and standard deviation are presented in Fig. 1. With Control sample, the compressive strength cured for 3, 7, 14, and 28 days were 14.4, 33.4, 40.9, and 43.4 MPa, respectively. The most increased degree of the development of compressive strength was observed between 3 and 7 days. Meanwhile, the compressive strength was generally reduced in samples with the inclusion of SAP and PVA. This phenomenon could be explained as follows. SAP initially absorbs moisture, resulting in a relatively low water–cement ratio, which allows excellent compressive strength to be obtained in the early stages. Specifically, the dense cement matrix induced by the initial water absorption of SAP and PVA is closely related to the high compressive strength, especially in the initial stage. However, the effect of lowering the water–cement ratio due to initial moisture absorption leads to initial strength development but can generally result in a later reduction in strength. Furthermore, the dense cement matrix induced by initially absorption of water in SAP and PVA was closely related to the high compressive strength especially in the early stage (Wong & Buenfeld, 2009). That is, while SAP may initially absorb a portion of the mixed water, SAP swollen in water can act as SAP-filled pores, significantly degrading mechanical properties (Kang et al., 2017; Kim et al., 2022).

In the meantime, water for full hydration reaction is insufficient due to the early water absorption by SAP. Therefore, compressive strength could not be sufficiently developed when the excessive amount of SAP and PVA increased by 0.03 wt.% and 0.5 wt.%, respectively (Kirby & Biernacki, 2012). This trend was observed continuously until 28 days. Therefore, rapid initial hardening was confirmed in the samples in which self-healing materials were adequately mixed. For the samples of S05F25 and S10F25, both the initial and later compressive strength have been confirmed.

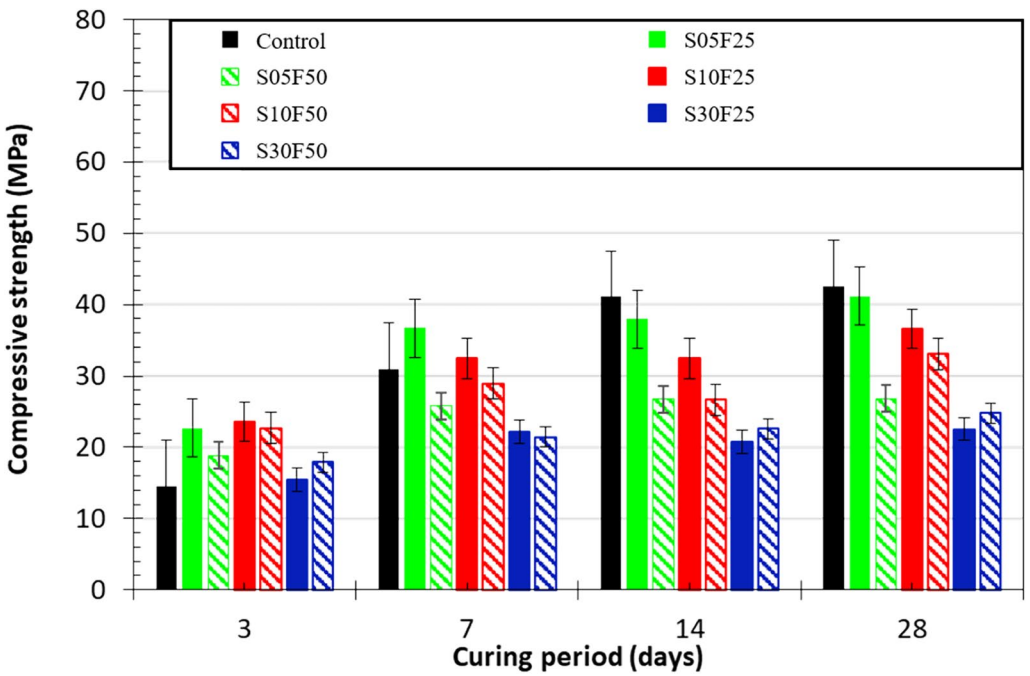

Fig. 1 Compressive strength results

3.2 Flexural Strength Results

The flexural strength was measured by three-point bending experiments. Except for S30F25 sample, the enhanced flexural strength was obtained compared to the Control sample (Fig. 2). In particular, an interesting trend was observed in the sample of S10F50. The flexural strength of the Control sample cured for 3 days was measured at 5.0 MPa, but the results of comparing the difference in flexural strength on the 3 and 28 days of curing according to the added amount of SAP and PVA are as follows. On the 3 days, the flexural strength of the S10F50 sample with 0.01 wt.% of SAP and 0.5 vol.% of PVA was 6.6 MPa. This showed that the flexural strength of the S10F50 sample was 31.2% higher than that of the Control sample. And on the 28 days of curing, the flexural strength of the Control sample and the S10F50 samples were 9.6 MPa and 8.5 MPa, respectively. In addition, it showed that the flexural strength of the S10F50 sample was 12.79% lower than that of the Control sample. Consequently, it was verified that the incorporation of a suitable quantity of SAP and PVA (i.e., S10F50) exerted a positive influence on the initial flexural strength of the developed cementitious system. However, this effect was observed to diminish somewhat in later stages. Nonetheless, when taking into account the error bars associated with the flexural strength measurements, it can be concluded that the flexural strength remained largely consistent.

3.3 Isothermal Calorimetry Results

The isothermal calorimetry analysis results are presented in Fig. 3. Since extra water was added to the sample contained SAP, a Control sample for S10F25 was additionally prepared; Control-No.4 was configured to have the same water-to-cement ratio except for SAP in the S10F25 to consider the effect of extra water. As the SAP incorporated, the heat of hydration decreased for 3 days. It is due to absorbed water by the SAP in initial hydration period which led to the reduction of mixing water for OPC hydration. As a result of comparing Control and Control-No.4, the cumulative heat of hydration slightly decreased with the extra water. Furthermore, as the content of SAP increased, the total amount of heat released between 10 and 30 h decreased. In this period, hydration behavior was prolonged, substantially. Therefore, it can be concluded that the inclusion of SAP has a retardation effect as a function of the dosage of those admixtures.

3.4 TGA Results

The TGA measurement results are shown in Fig. 4a–g. In all samples, similar trend was confirmed. Firstly, the calculated CBW values increased as the curing duration increased. It indicated that the hydration reactions continuously occurred, and the increased hydration products [e.g., AFm, AFt, and calcium-silicate-hydrated (C–S–H)] could be confirmed as curing duration increased (Pane & Hansen, 2005; Wang et al., 2020). The main weight

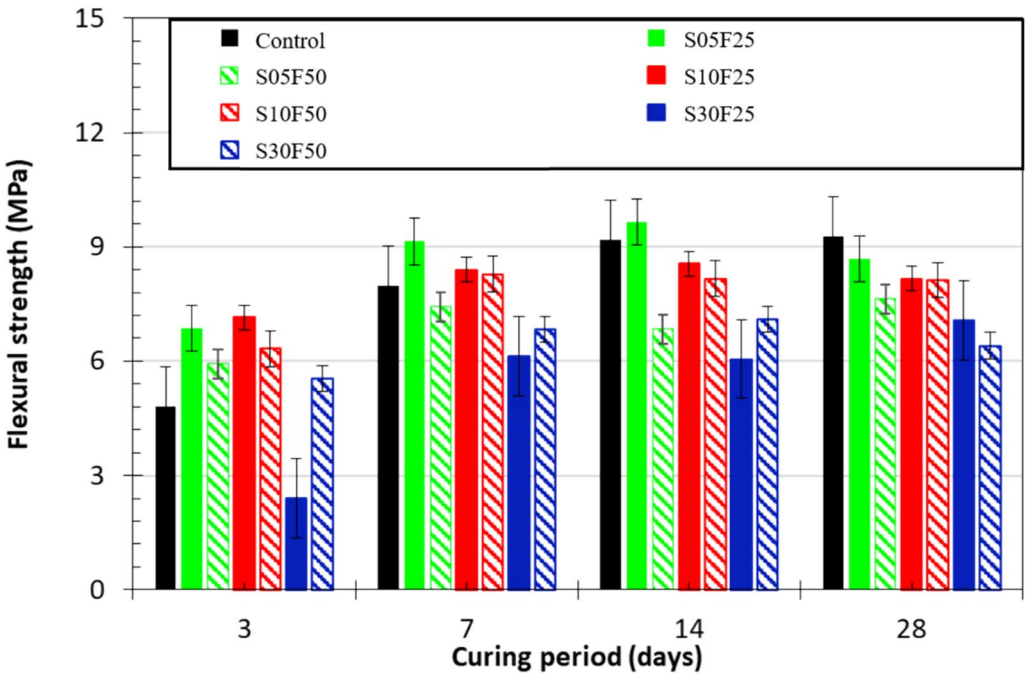

Fig. 2 Flexural strength results

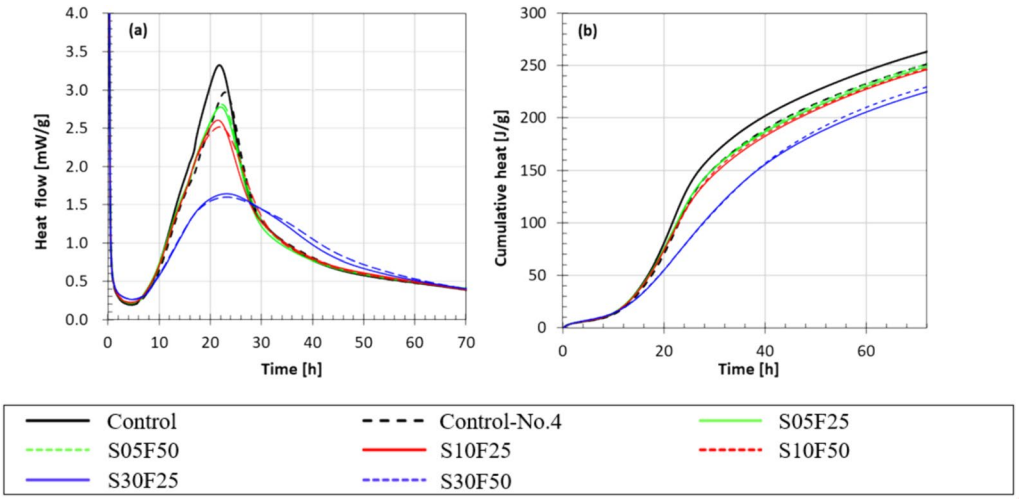

Fig. 3 Hydration heat evolution of OPC according to the content of SAP and PVA: **a** heat flow and **b** cumulative heat flow

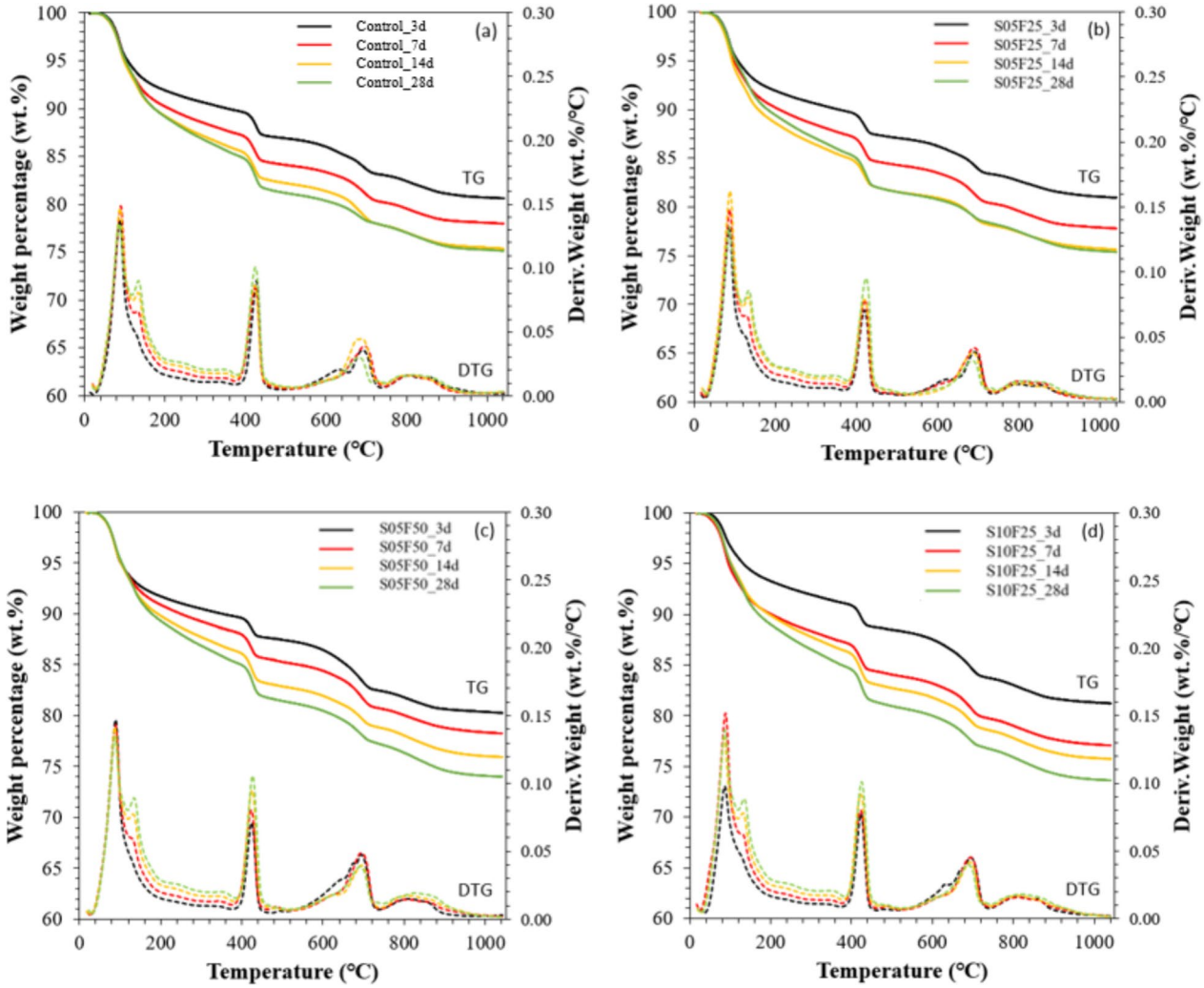

Fig. 4 TGA results: samples. **a** Control, **b** S05F25, **c** S05F50, **d** S10F25, **e** S10F50, **f** S30F25, and **g** S30F50

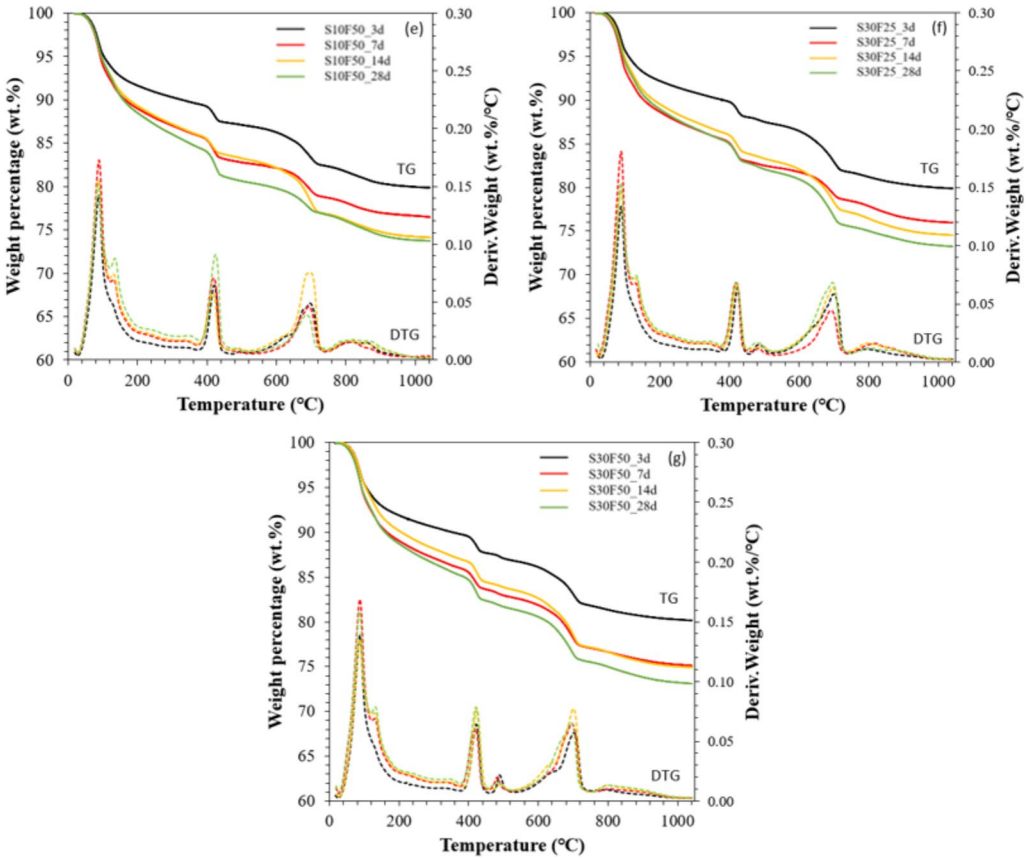

Fig. 4 continued

loss occurred between 400 and 500 °C, which indicated that the pyrolysis of calcium hydroxide, the amount of calcium hydroxide was also augmented. However, the amount of calcium carbonate was generally maintained according to the curing, which indicated that the carbonation effect was not occurred in this study (Ho et al., 2018).

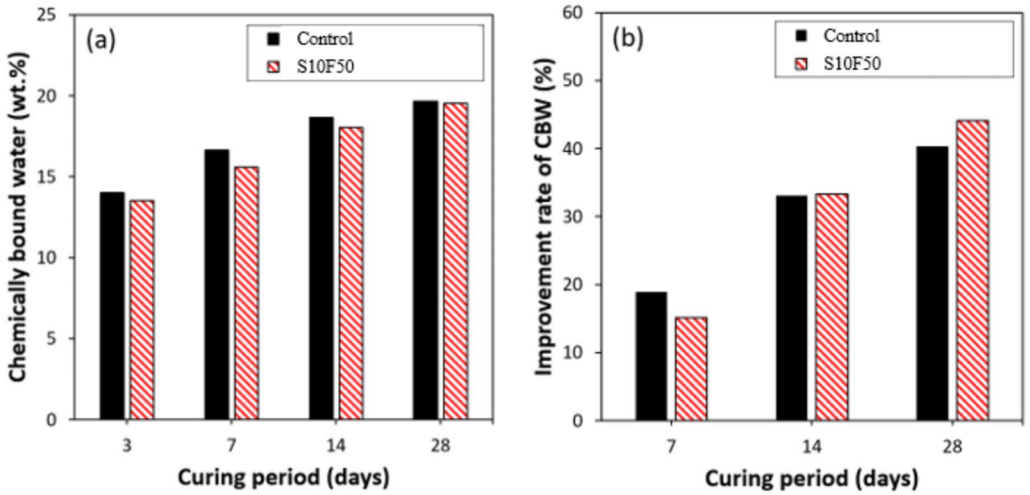

Fig. 5 Analysis of TGA results: **a** the weight percentage of chemically bound water of Control and S10F50 samples and **b** improvement rate of CBW compared to 3 days of curing in each mix design

As shown in Fig. 5a, the CBW values of S10F50 sample were lower than those of the Control sample. Meanwhile, the difference between those was reduced as the curing proceeded. In each mix proportion, the improvement rate of CBW according to the curing days compared to that of 3 days of curing is shown in Fig. 5b. The CBW improvement rate of the self-healing mixture was lower than that of the Control at the early age; this retardation effect was also confirmed in the results of the isothermal calorimetry test. However, it significantly increased at 28 days of curing, surpassing the CBW improvement rate of the Control sample. It indicated that the internal curing effect actively occurred in the sample. As summarized, additional hydration reaction (i.e., internal curing effect) actively occurred from 7 to 28 days. Therefore, it can be confirmed that more water content was initially absorbed as the SAP was helpful, and as the water released over time, the secondary hydration which is called self-healing effect was activated.

3.5 XRD Results

The measured XRD patterns for all variables are shown in Fig. 6. In this study, basic hydration mechanism has not been substantially modified using dual admixtures. In Fig. 6, the AFt and AFm phases were observed in a 2Θ range from 6 to 14°. In particular, when the curing date increased, the increased amount of AFm phase was observed in all samples investigated. However, trivial differences were observed depending on the variables. In addition, the amount of AFm formed differed according to the content of SAP and PVA. The hydration mechanism was slightly changed when the SAP and PVA were added. Except for the samples of Control and S10F50, the aluminate reaction increased in the later stage. Furthermore, the solid solution having hemicarbonate phase was observed in the certain sample; in the samples of S10F50-7 days and S30F25-28 days, the peak located in 11° at 2Θ was clearly confirmed (Nedyalkova et al., 2020).

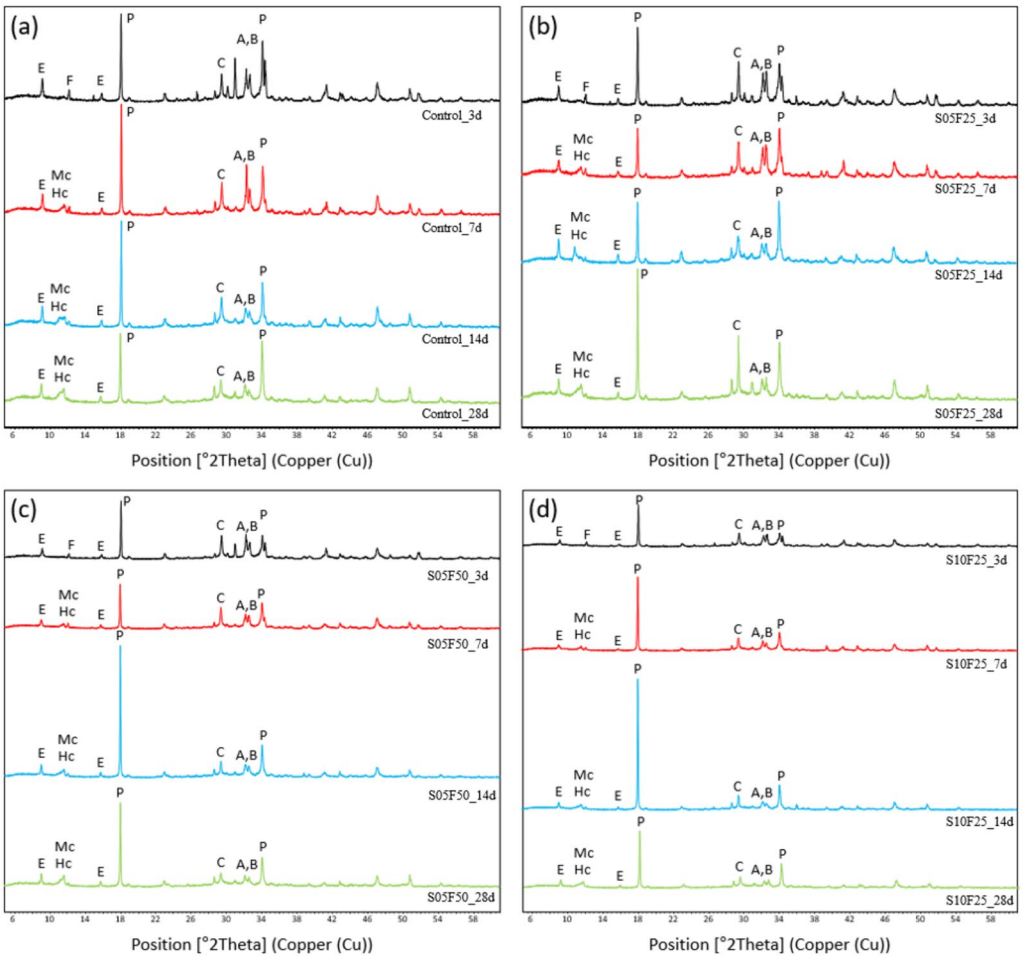

Fig. 6 XRD results: samples. **a** Control, **b** S05F25, **c** S05F50, **d** S10F25, **e** S10F50, **f** S30F25, and **g** S30F50

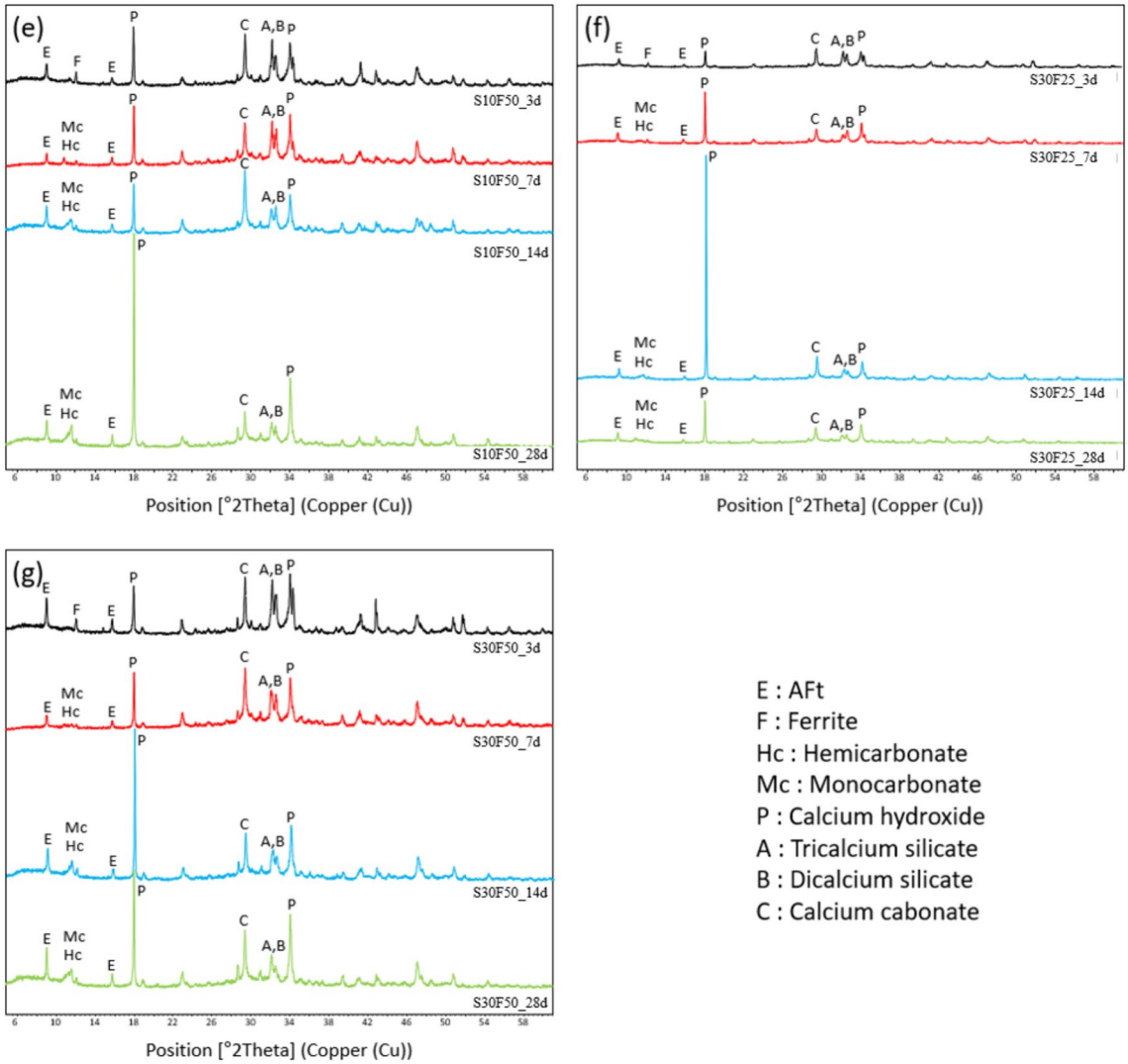

Fig. 6 continued

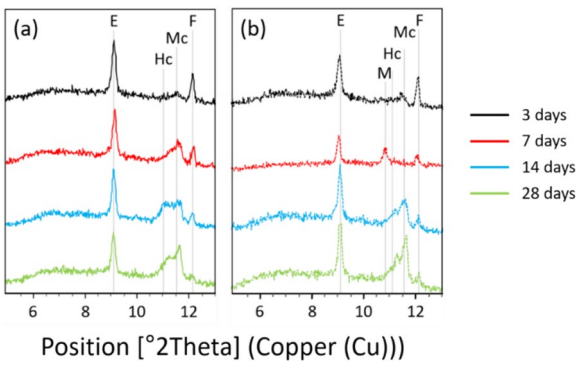

Fig. 7 XRD measurement results of Control (**a**) and S30F25 (**b**) samples: E, Hc, Mc, F, and M indicates ettringite, hemicarbonate, monocarbonate, ferrite, and AFm phase, respectively

As mentioned in prior section, interesting results were observed in the XRD analysis; in the specific samples, the different AFm phase was confirmed (Fig. 7). This phenomenon could be explained as follows. The crystallographic properties of AFm phase series could be easily changed depending on the environment in which it is formed as a solid solution (Balonis et al., 2010; Mesbah et al., 2011). In other words, when the SAP and PVA were applied, the environment of the cement matrix could be significantly changed owing to the relative humidity variation induced by the excellent water absorption properties (Mudiyanselage & Neckers, 2008). Furthermore, the increased amount of

monocarbonate was also observed in the S10F50 sample. Hence, the variations of AFm phase could be the evidence of the internal curing effect induced using SAP or PVA or both.

3.6 Micro-CT Results

The self-healing performance on the intended crack was confirmed using a micro-CT. The crack width image of one cross-section through CT is shown in Fig. 8, and the entire crack surface is shown in Fig. 9. Additionally, the

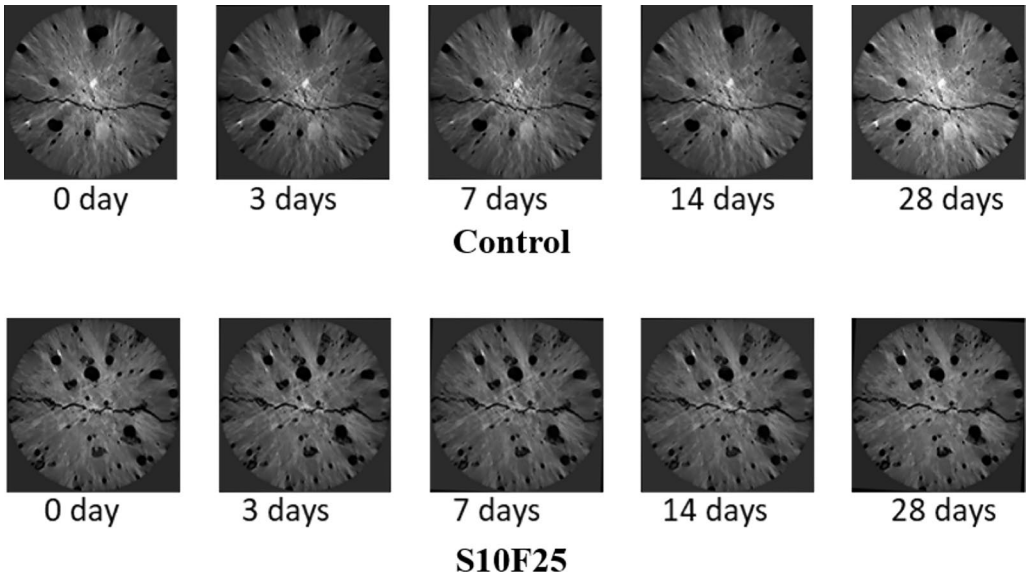

Fig. 8 Micro-CT measurement results

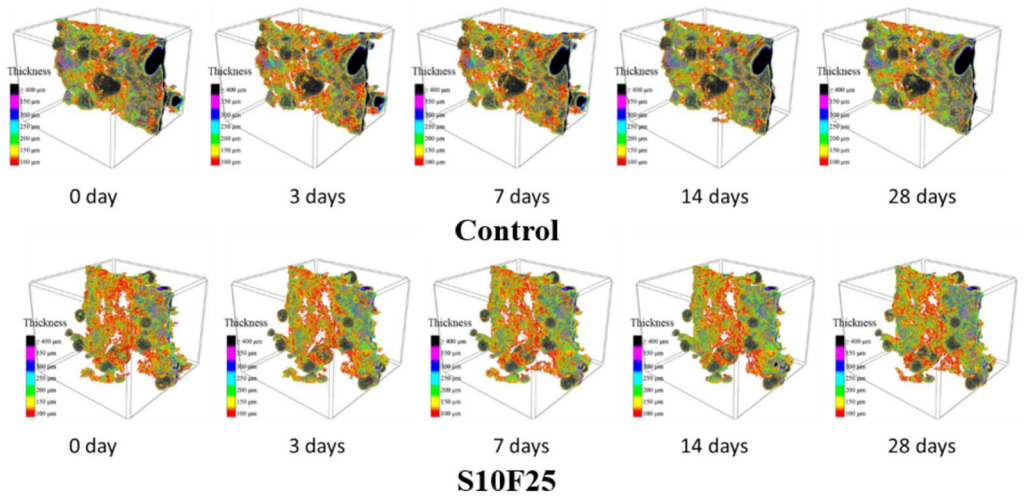

Fig. 9. 3 dimensions rendering results

Table 3 Crack volume analysis according to the curing days

No.	Notation	Crack volume percentage (%)				
		0 day	3 days	7 days	14 days	28 days
1	Control	2.82	2.75	2.58	2.51	2.09
2	S10F25	5.12	5.08	4.98	4.21	4.08

volume of entire crack width with respect to the volume of interest (VOI) scanned through CT was converted into percentage and shown in Table 3. With the Control sample, a remarkable degree of self-healing effect was observed at the specific durations (until 14 days), but it is difficult to confirm the self-healing effect between 14 and 28 days. Meanwhile, a different trend was observed in the S10F25 sample. That is, the self-healing effect was clearly expressed a lot between 14 and 28 days.

3.7 Optical Microscopy Measurement Results

The crack width measurement results using optical microscopy are presented in Fig. 10. It was visually confirmed that the crack width is well controlled on the surface of the crack and was filled by the self-healing material. Fig. 11 shows the normalized crack width according to self-healing performance. In all mix design, the crack width decreased rapidly at the early stages. With Control sample, as the initially controlled crack width widened, the self-healing effect was significantly lower than that of other mixtures. In particular, the control sample with a crack width of 300 μm maintained about 60% of the initially introduced crack even after curing for 91 days. On the other hand, in all self-healing mortars, the crack tended to decrease as the mixing amount of SAP and PVA increased.

3.8 Leaking Test Results

The results of the leaking test are presented in Fig. 12. In the case of Control sample, the normalized water amount increased with the crack width increase. Significant normalized water content was observed despite the sample being cured for 91 days in the Control sample with a crack width of 300 μm. This trend was similar to the results of crack width measurement. In addition, the lower normalized water amount of the sample with SAP and PVA was confirmed in the later stage. Especially, as the crack gradually filled with self-healing material, the amount of water leaked over a period of 30 min was greatly reduced. As mentioned above, the self-healing abilities of SAP and PVA for a quite wide crack width are also extensively supported.

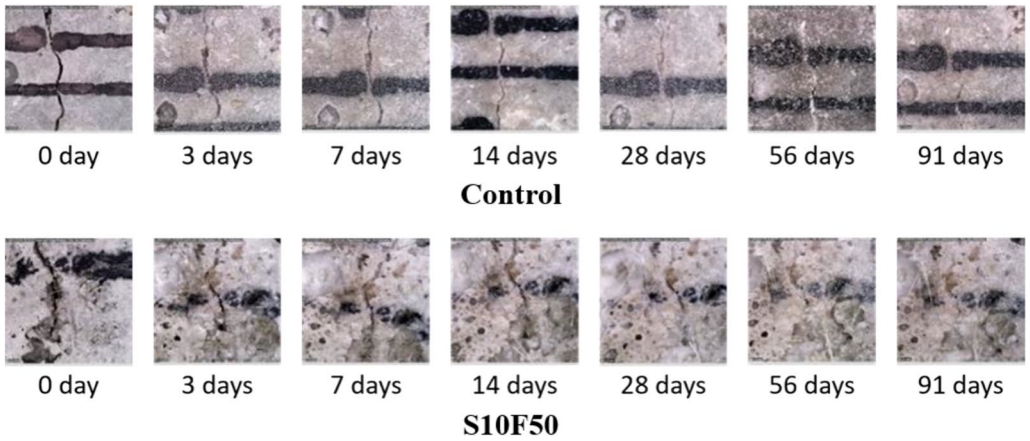

Fig. 10 Optical microscopy measurement results (measured area in the photo: 7.651 mm × 5.596 mm)

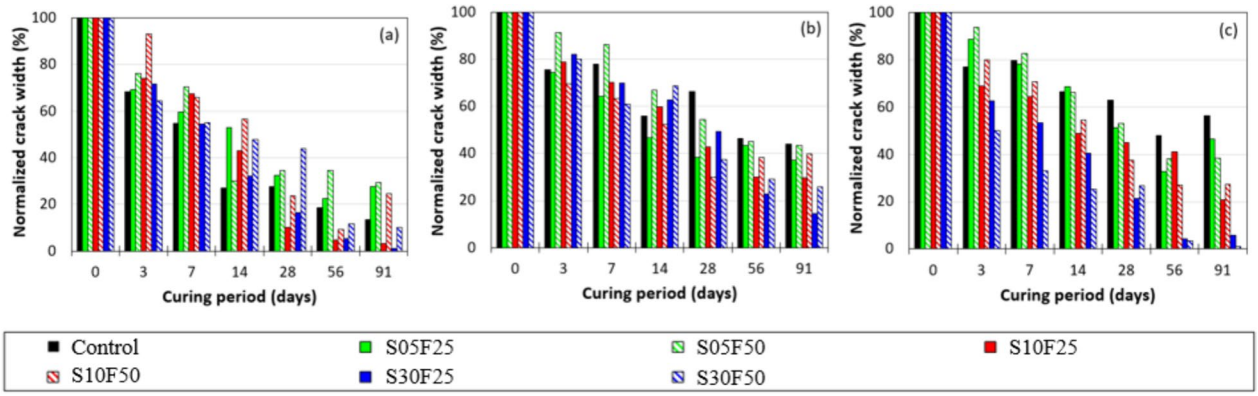

Fig. 11 Results of the optical microscopy measurement: **a** 100 μm of crack width, **b** 200 μm of crack width, and **c** 300 μm of crack width

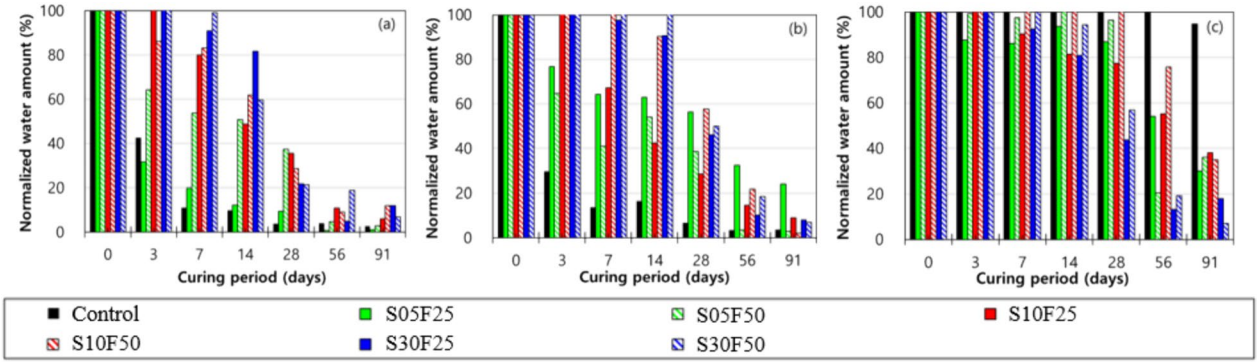

Fig. 12 Results of the leaking test: **a** 100 µm of crack width, **b** 200 µm of crack width, and **c** 300 µm of crack width

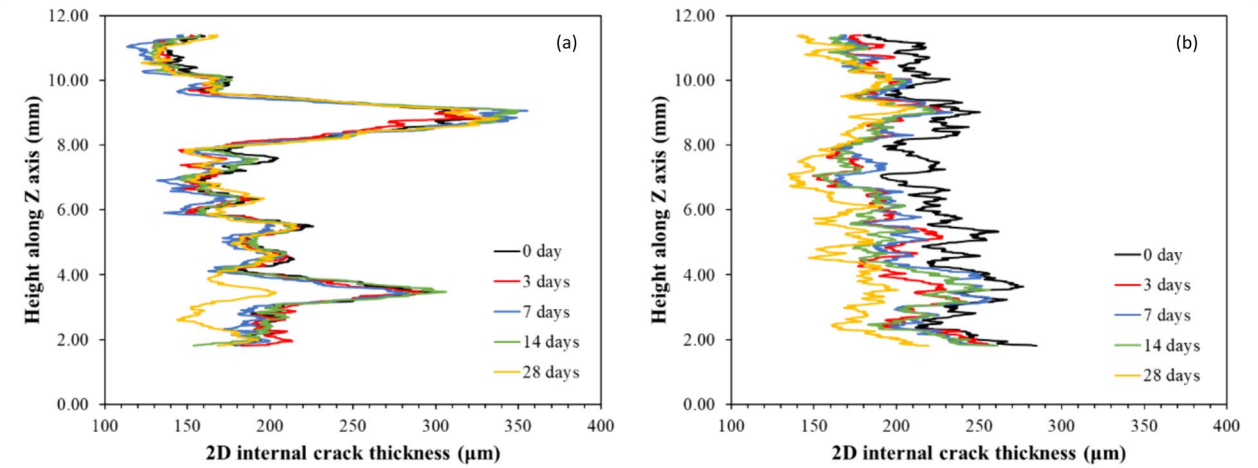

Fig. 13. 3-dimensional rendering results through micro-CT: **a** Control and **b** S30F25

4 Discussion

4.1 Improved Self-healing Effects According to the SAP and PVA

Fig. 13 shows the results of 3-dimensional rendering through micro-CT based on the crack thickness and crack volume analysis results. The results of analyzing the cracks in the self-healing mortar sample through 3 dimensions tomography are as follows. In the case of the Control sample with a crack width of 200 µm, the self-healing effect was hardly confirmed at the early stage, but it was clearly observed between 14 and 28 days. On the other hand, with the S30F25 sample containing SAP and PVA, the effect was generally high, and this phenomenon was the most pronounced in the sample containing 3 wt.% of SAP. Therefore, it can be concluded that the use of dual admixture of SAP and PVA enhances the self-healing performance in the designed cementitious system.

Through the crack width measurement and leakage test of the self-healing mortar for 91 days, self-healing effect was evaluated by calculating the healing rate of both crack width (HR_{CW}) and leaking water test (HR_{LW}). The HR_{CW} of each variable was calculated using Eq. 1, where W_0, t, and W_t indicated that the crack width at 0 day, self-healing curing date after crack introduction, and crack width at t day(s), respectively:

$$HR_{CW} = \frac{W_0 - W_t}{W_0} \times 100[\%]. \quad (1)$$

The HR_{LW} was calculated using the following Eq. 2, where w_0, t, and w_t indicated that the amount of leaked water at 0-day, self-healing curing date after crack introduction, and the amount of leaked water on t day(s), respectively:

$$HR_{LW} = \frac{w_0 - w_t}{w_0} \times 100[\%]. \quad (2)$$

The healing rate for crack width of samples with SAP and PVA were higher than that of Control sample. In particular, when the crack width increased, the reduction of self-healing performance was observed in the Control sample. The improved HR_{CW} was observed when the added amount of SAP and PVA increased regardless of the crack widths (Fig. 14). It indicated that the combination of SAP and PVA maximize the self-healing effect in the cement matrix. It should be noted here that the HR_{CW} of samples of S10F50 and S30F50 is higher than other samples. The self-healing performance of the fore-mentioned samples was the highest in all widths, which is due to the incorporation of a significant amount of PVA fiber. Although SAP also contributes to the self-healing effect, in the case of PVA fiber, it showed a surprising increase in self-healing performance because it adheres to cracks and allows the formation of self-healing products (Park & Choi, 2018). In the case of Control sample with a crack width of 300 μm, the HR_{CW} in lower than 60% on all curing dates. Meanwhile, when the proper amount of SAP and PVA was applied, the HR_{CW} was approaching 100% at 91 days. These results strongly support that the self-healing performance of SAP and PVA for relatively wide crack widths are evident.

As shown in Fig. 15a and b, the HR_{LW} of Control sample with crack widths of 100 and 200 μm dramatically increased until 7 days. However, the self-healing effect was not observed in the Control sample with a crack width of 300 μm. Instead, the self-healing effect was confirmed in the samples containing SAP and PVA, and in particular, the effect was strengthened as the content of SAP increased (Fig. 15c). The discrepancy between the results of the leaking test and optical microscopy measurement might have originated from the measurement site. That is, in the case of optical microscopy measurement, the upper end of the specimen was measured locally, but in the case of the leaking test, the water flow inside the specimen was measured.

5 Summary and Conclusions

This study elucidated that the newly developed cementitious composite with SAP and PVC fiber has self-healing ability and suitable mechanical performance. The self-healing performance was evaluated with the micro-CT, leaking test, and optical microscopy measurement. In addition, the self-healing hydration mechanism of OPC accompanying the SAP and PVA were studied based on the XRD, TGA, and isothermal calorimetry methods. The conclusion of this study is as follows:

For narrow cracks (100 μm), the self-healing materials showed lower crack healing ratios (CHRs) compared to the Control sample. However, for wider cracks (200 and 300 μm), samples with SAP and PVA exhibited excellent self-healing performance. The used materials absorbed and slowly released water, resulting self-healing and internal curing effects. Initially, the water absorption led to higher compressive and flexural strength (up to 3 days), possibly due to the effect of reduction of water-to-cement ratio. Subsequently, the control sample showed the highest increase in mechanical properties from 3 to 14 days. Compared to other cementitious systems with dual admixtures, the S10F50 sample displayed improved mechanical properties due to the internal curing effect.

In the TGA, XRD, and heat flow results, the control sample showed accelerated OPC hydration in the early stage (up to 3 days). In contrast, the addition of SAP and PVA

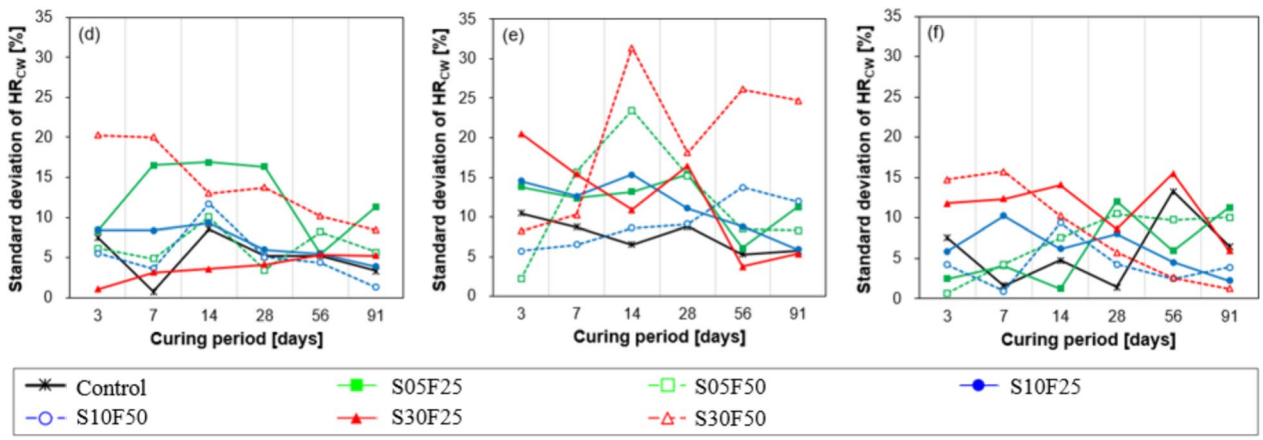

Fig. 14 Self-healing performance evaluation results using the microscopy measurements: **a** 100 μm of crack width, **b** 200 μm of crack width, **c** 300 μm of crack width, **d** standard deviation of HR_{CW} (100 μm), **e** standard deviation of HR_{CW} (200 μm), and **f** standard deviation of HR_{CW} (300 μm)

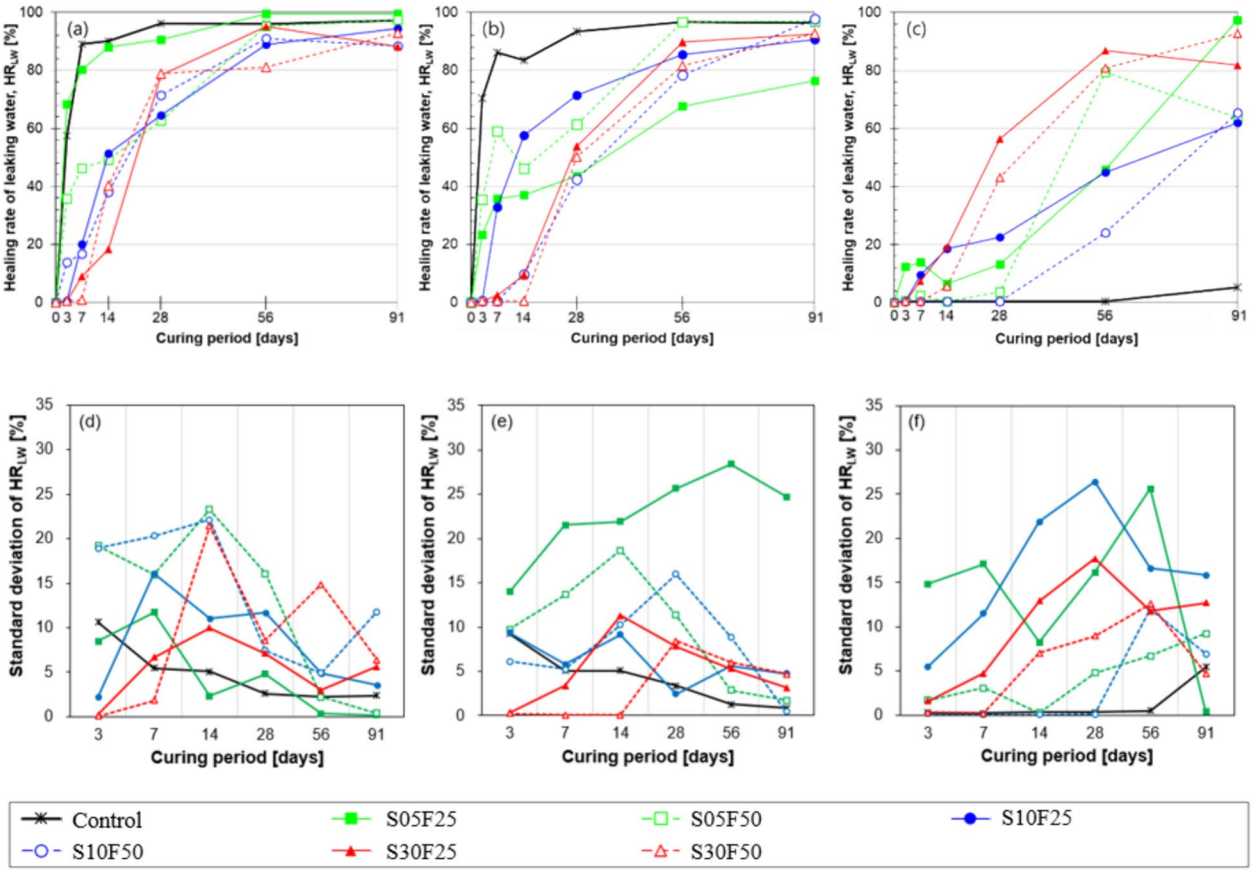

Fig. 15 Self-healing performance evaluation results based on the leaking tests: **a** 100 μm of crack width, **b** 200 μm of crack width, **c** 300 μm of crack width, **d** standard deviation of HR_{LW} (100 μm), **e** standard deviation of HR_{LW} (200 μm), and **f** standard deviation of HR_{LW} (300 μm)

(S10F50) resulted in an anomalous hydration reaction compared to the Control sample. Most of the AFt phase was formed in the Control sample before 3 days, with little change after 3 days. However, in samples with SAP and PVA, significant AFt phase formation occurred between 7 and 14 days, along with the remarkable formation of hydration products attributed to the internal curing effect in the later stage.

Acknowledgements
The research described in this paper was supported by Korea Land and Housing Corporation (project No. R202003005). The authors are grateful to the sponsors for the financial supports.

Author contributions
S. Kwon & S. Lee: conceptualization, writing—reviewing and editing. H. Kang, M. Kim, S. Her: investigation, data curation, formal analysis, visualization, writing—original draft. S. Bae, D. Kim & J. Moon: conceptualization, writing—reviewing and editing.

Funding
The research described in this paper was supported by Korea Land and Housing Corporation (project No. R202003005).

Availability of data and materials
All the datasets associated with this study are available from the corresponding author upon request.

Declarations

Ethics approval and consent to participate
All authors of the manuscript confirm the ethics approval and consent to participate following the Journal's policies.

Consent for publication
All authors of the manuscript agree on the publication of this work in the *International Journal of Concrete Structures and Materials*.

Competing interests
The authors declare no conflict of interest.

Received: 10 March 2023 Accepted: 28 April 2024
Published online: 16 August 2024

References

Balonis, M., Lothenbach, B., Le Saout, G., & Glasser, F. P. (2010). Impact of chloride on the mineralogy of hydrated Portland cement systems. *Cement and Concrete Research, 40*(7), 1009–1022.

Branco, F. A., & Mendes, P. A. (1993). Thermal actions for concrete bridge design. *Journal of Structural Engineering, 119*(8), 2313–2331.

Chindasiriphan, P., Yokota, H., & Pimpakan, P. (2020). Effect of fly ash and superabsorbent polymer on concrete self-healing ability. *Construction and Building Materials, 233*, 116975.

Deboucha, W., Leklou, N., Khelidj, A., & Oudjit, M. N. (2017). Hydration development of mineral additives blended cement using thermogravimetric analysis (TGA): Methodology of calculating the degree of hydration. *Construction and Building Materials, 146*, 687–701.

Gagg, C. R. (2014). Cement and concrete as an engineering material: An historic appraisal and case study analysis. *Engineering Failure Analysis, 40*, 114–140.

Gardner, D., Lark, R., Jefferson, T., & Davies, R. (2018). A survey on problems encountered in current concrete construction and the potential benefits of self-healing cementitious materials. *Case Studies in Construction Materials, 8*, 238–247.

Gustavsson, L., & Sathre, R. (2006). Variability in energy and carbon dioxide balances of wood and concrete building materials. *Building and Environment, 41*(7), 940–951.

Ho, L. S., Nakarai, K., Ogawa, Y., Sasaki, T., & Morioka, M. (2018). Effect of internal water content on carbonation progress in cement-treated sand and effect of carbonation on compressive strength. *Cement and Concrete Composites, 85*, 9–21.

Homma, D., Mihashi, H., & Nishiwaki, T. (2009). Self-healing capability of fibre reinforced cementitious composites. *Journal of Advanced Concrete Technology, 7*(2), 217–228.

Jacobsen, S., & Sellevold, E. J. (1996). Self healing of high strength concrete after deterioration by freeze/thaw. *Cement and Concrete Research, 26*(1), 55–62.

Jansen, D., Goetz-Neunhoeffer, F., Lothenbach, B., & Neubauer, J. (2012). The early hydration of Ordinary Portland Cement (OPC): An approach comparing measured heat flow with calculated heat flow from QXRD. *Cement and Concrete Research, 42*(1), 134–138.

Jensen, O. M., & Hansen, P. F. (2002). Water-entrained cement-based materials: II. Experimental Observations. *Cement and Concrete Research, 32*(6), 973–978.

Jeong, Y., Hargis, C. W., Chun, S. C., & Moon, J. (2018). The effect of water and gypsum content on strätlingite formation in calcium sulfoaluminate-belite cement pastes. *Construction and Building Materials, 166*, 712–722.

Jeong, Y., Kang, S. H., Du, Y., & Moon, J. (2019). Local Ca-structure variation and microstructural characteristics on one-part activated slag system with various activators. *Cement and Concrete Composites, 102*, 1–13.

Jeong, Y., Park, H., Jun, Y., Jeong, J. H., & Oh, J. E. (2015). Microstructural verification of the strength performance of ternary blended cement systems with high volumes of fly ash and GGBFS. *Construction and Building Materials, 95*, 96–107.

Jonkers, H. M., Thijssen, A., Muyzer, G., Copuroglu, O., & Schlangen, E. (2010). Application of bacteria as self-healing agent for the development of sustainable concrete. *Ecological Engineering, 36*(2), 230–235.

Joseph, C., A. Jefferson, and M. Cantoni. (2007). *Issues relating to the autonomic healing of cementitious materials*. in *First international conference on self-healing materials*.

Kang, H., & Moon, J. (2021). Secondary curing effect on the hydration of ultra-high performance concrete. *Construction and Building Materials, 298*, 123874.

Kang, S.-H., Hong, S.-G., & Moon, J. (2017). Absorption kinetics of superabsorbent polymers (SAP) in various cement-based solutions. *Cement and Concrete Research, 97*, 73–83.

Kang, S. H., Kang, H., Lee, N., Kwon, Y. H., & Moon, J. (2022). Development of cementless ultra-high performance fly ash composite (UHPFC) using nucleated pozzolanic reaction of low Ca fly ash. *Cement and Concrete Composites, 132*, 104650.

Kang, S. H., Kwon, M., Kwon, Y. H., & Moon, J. (2021). Effects of polycarboxylate ether (PCE)-based superplasticizer on the dissolution and subsequent hydration of calcium oxide (CaO). *Cement and Concrete Research, 146*, 106467.

Kim, M., J. Moon, and S.-G. Hong. (2022). *Theoretical study on the freeze resistance of concrete mixed with superabsorbent polymer (SAP) considering the reabsorption behavior of SAP.* Journal of Sustainable Cement-Based Materials, p. 1–13.

Kirby, D. M., & Biernacki, J. J. (2012). The effect of water-to-cement ratio on the hydration kinetics of tricalcium silicate cements: Testing the two-step hydration hypothesis. *Cement and Concrete Research, 42*(8), 1147–1156.

Lee, H., Wong, H., & Buenfeld, N. (2010). Potential of superabsorbent polymer for self-sealing cracks in concrete. *Advances in Applied Ceramics, 109*(5), 296–302.

Lee, H., Wong, H., & Buenfeld, N. (2016). Self-sealing of cracks in concrete using superabsorbent polymers. *Cement and Concrete Research, 79*, 194–208.

Li, M., & Li, V. C. (2011). Cracking and healing of engineered cementitious composites under chloride environment. *ACI Materials Journal, 108*(3), 333.

Li, V. C., Lim, Y. M., & Chan, Y.-W. (1998). Feasibility study of a passive smart self-healing cementitious composite. *Composites Part B: Engineering, 29*(6), 819–827.

Li, V. C., Wu, C., Wang, S., Ogawa, A., & Saito, T. (2002). Interface tailoring for strain-hardening polyvinyl alcohol-engineered cementitious composite (PVA-ECC). *Materials Journal, 99*(5), 463–472.

Mesbah, A., Cau-dit-Coumes, C., Frizon, F., Leroux, F., Ravaux, J., & Renaudin, G. (2011). A new investigation of the Cl−–CO32− substitution in AFm phases. *Journal of the American Ceramic Society, 94*(6), 1901–1910.

Mihashi, H., Kaneko, Y., Nishiwaki, T., & Otsuka, K. (2000). Fundamental study on development of intelligent concrete characterized by self-healing capability for strength. *Transactions of the Japan Concrete Institute, 22*, 441–450.

Mudiyanselage, T. K., & Neckers, D. C. (2008). Highly absorbing superabsorbent polymer. *Journal of Polymer Science Part a: Polymer Chemistry, 46*(4), 1357–1364.

Nasim, M., Dewangan, U., & Deo, S. V. (2020). Effect of crystalline admixture, fly ash, and PVA fiber on self-healing capacity of concrete. *Materials Today: Proceedings, 32*, 844–849.

Nedyalkova, L., Lothenbach, B., Geng, G., Mäder, U., & Tits, J. (2020). Uptake of iodide by calcium aluminate phases (AFm phases). *Applied Geochemistry, 116*, 104559.

Pae, J., Kang, S. H., Lee, N., Kim, S., & Moon, J. (2021b). Flow distance induced variation analysis of digitally segmented steel fibers in UHPFRC. *Construction and Building Materials, 303*, 124515.

Pae, J., Zhang, Y., Poh, L. H., & Moon, J. (2021a). Three-dimensional transport properties of mortar with a high water-to-cement ratio using X-ray computed tomography. *Construction and Building Materials, 281*, 122608.

Pane, I., & Hansen, W. (2005). Investigation of blended cement hydration by isothermal calorimetry and thermal analysis. *Cement and Concrete Research, 35*(6), 1155–1164.

Park, B., & Choi, Y. C. (2018). Quantitative evaluation of crack self-healing in cement-based materials by absorption test. *Construction and Building Materials, 184*, 1–10.

Reinhardt, H.-W., & Jooss, M. (2003). Permeability and self-healing of cracked concrete as a function of temperature and crack width. *Cement and Concrete Research, 33*(7), 981–985.

Şahmaran, M., & Li, V. C. (2009). Durability properties of micro-cracked ECC containing high volumes fly ash. *Cement and Concrete Research, 39*(11), 1033–1043.

Shin, J.-W., Her, S.-W., & Bae, S.-C. (2020). Investigation on the self-healing performance of cement mortar incorporating inorganic expansive additives. *Journal of the Korean Recycled Construction Resources Institute, 8*(4), 404–412.

Snoeck, D., Steuperaert, S., Van Tittelboom, K., Dubruel, P., & De Belie, N. (2012). Visualization of water penetration in cementitious materials with superabsorbent polymers by means of neutron radiography. *Cement and Concrete Research, 42*(8), 1113–1121.

Stewart, M. G., Wang, X., & Nguyen, M. N. (2011). Climate change impact and risks of concrete infrastructure deterioration. *Engineering Structures, 33*(4), 1326–1337.

Talaiekhozani, A., & Abd Majid, M. Z. (2014). A review of self-healing concrete research development. *Journal of Environmental Treatment Techniques, 2*(1), 1–11.

Termkhajornkit, P., Nawa, T., & Kurumisawa, K. (2006). Effect of water curing conditions on the hydration degree and compressive strengths of fly ash–cement paste. *Cement and Concrete Composites, 28*(9), 781–789.

Van Tittelboom, K., & De Belie, N. (2013). Self-healing in cementitious materials—A review. *Materials, 6*(6), 2182–2217.

Van Tittelboom, K., De Belie, N., Van Loo, D., & Jacobs, P. (2011). Self-healing efficiency of cementitious materials containing tubular capsules filled with healing agent. *Cement and Concrete Composites, 33*(4), 497–505.

Van Tittelboom, K., De Belie, N., De Muynck, W., & Verstraete, W. (2010). Use of bacteria to repair cracks in concrete. *Cement and Concrete Research, 40*(1), 157–166.
Wang, R., Yu, J., Gu, S., Han, X., He, P., Liu, Q., & Xue, L. (2020). Effect of ion chelator on hydration process of Portland cement. *Construction and Building Materials, 259*, 119727.
Wong, H., & Buenfeld, N. (2009). Determining the water–cement ratio, cement content, water content and degree of hydration of hardened cement paste: Method development and validation on paste samples. *Cement and Concrete Research, 39*(10), 957–965.
Yang, Y., Lepech, M. D., Yang, E. H., & Li, V. C. (2009). Autogenous healing of engineered cementitious composites under wet–dry cycles. *Cement and Concrete Research, 39*(5), 382–390.

Publisher's Note

Sukmin Kwon First Author, Researcher of Land and Housing Institute, Daejeon, Korea, 34047

Sugyu Lee Second Author, Researcher of Land and Housing Institute, Daejeon, Korea, 34047

Hyunuk Kang Third Author, PhD student in Seoul National University, Seoul, Korea, 08826

Min Kyoung Kim Forth Author, Post-doc researcher in Sejong University, Seoul, Korea, 05006

Sungwun Her Fifth Author, PhD student in Hanyang University, Seoul, Korea, 04763

Sungchul Bae Sixth Author, Associate Professor in Hanyang University, Seoul, Korea, 04763

Dong Joo Kim Seventh Author, Professor in Sejong University, Seoul, Korea, 05006

Juhyuk Moon Corresponding Author, Associate Professor in Seoul National University, Seoul, Korea, 08826